3.1 Introduction

Any fluid flow is governed by three fundamental conservation laws, i.e., conservation of mass, conservation of momentum and conservation of energy. Governing equations for fluid flow are derived from the mathematical formulation of these laws. These governing equations are either in the form of partial differential equations or integral equations.

Partial differential equations are obtained if the governing equations are applied to an infinitesimal fluid particle moving within the flow, whereas the integral form of the governing equations is applied if the conservation laws are applied to a fixed volume in the flow domain. The equations are coupled and nonlinear in either of the cases, which can then be solved.

The governing equations are solved approximately on the computer using the software in computational fluid dynamics or CFD. The overview of this black box model is presented in Fig. 3.1. The CFD software converts the governing equations to a large set of algebraic equations using numerical methods. The large set of algebraic equations is inverted to get the cell center values. With recent advances in CFD technology, flow around realistic geometries and complex physics can be handled, thus saving project cost and time.

The CFD software used in this present study will be ANSYS Fluent from ANSYS Incorporated, a leading, general-purpose CFD solver used in the industry.

ANSYS Fluent solves the governing equations for fluid flow using a numerical technique called the finite volume method (FVM).

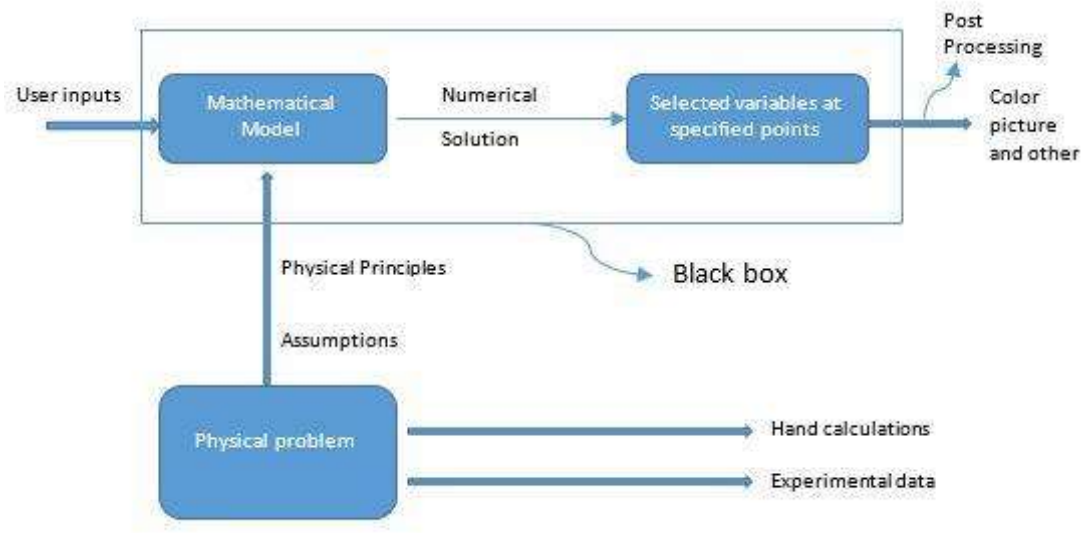

Figure 3. 1 Overview of Black Box Model (Courtesy of A Hands-on Introduction to Engineering Simulations (edX) by Dr.Rajesh Bhaskaran)

FVM technique allows the entire flow domain in a large number of small control volumes. The conservation equations are applied in these control volumes using the integral form of the governing equations, giving us a set of algebraic equations.

The Finite Volume Method (FVM) is preferred in CFD applications over the Finite element method (FEM) because the conservation equations are applied directly rather than indirectly. The quantities in each control volume are conserved in a discreet sense.

The numerical methodology of solving a problem consists of creating a mathematical model with assigned governing equations and boundary conditions.

3.2 Mathematical model

Flow-through a weir is unsteady in nature. A half key 3D PKW model has been used throughout the Thesis with the geometry of the physical experimental models.

The mathematical model consists of governing equations and boundary conditions, which are discussed below.

3.3 Governing Equations

ANSYS FLUENT solves mass, momentum and energy conservation equations for all flows. The governing equations are depicted in Table 3.1 below.

Table 3. 1 Conservation of mass and momentum equations

Sl. No.		Differential form	Integral form
1.	Conservation of mass	$\nabla.\vec{V} = 0$	$\int_S \vec{V} \cdot \hat{n}\, dS = 0$
2.	Conservation of Momentum	$\rho(\vec{V} \cdot \nabla)\vec{V}$ $= -\nabla\rho + \mu\nabla^2\vec{V}$	$\int_S \rho\vec{V}(\vec{V} \cdot \hat{n})\, ds$ $= \int_S p\, \hat{n}\, ds$ $+ \vec{F}_{visc}$

The first equation is the conservation of mass or the continuity equation. The law of mass conservation implies that the volume of a fluid particle moving within the flow cannot change or the net volume flow out of any arbitrary control volume has to be zero.

The second equation is the conservation of momentum, which represents the net pressure force on an infinitesimal fluid particle. It represents the net viscous friction or viscous shear on the infinitesimal fluid particle per unit volume. The governing equations are defined in a particular domain of the mathematical model in the present study.

3.4 Boundary conditions

The boundary conditions are defined at the edges of the domain. The simulations in the present study were performed on a 20 core CPU with the use of a parallel solver option

and double precision. Half PKW unit was used to model the flow in a channel, the channel dimensions being the one used in the experimental study. The boundary conditions used in the present study are depicted in Fig. 3.2 below. The water inlet boundary was located at a sufficient distance (~ 19 P) for developing uniform flow conditions for the above numerical study.

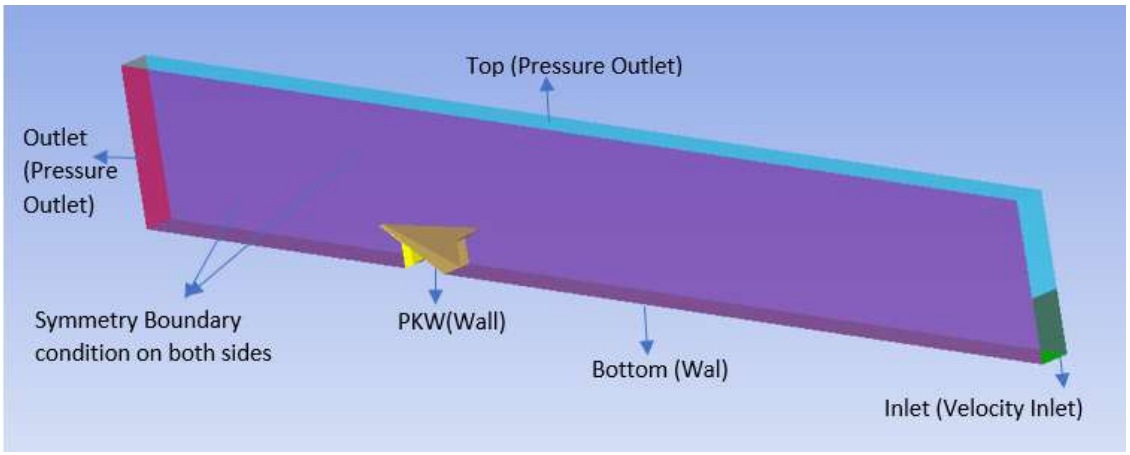

Figure 3. 2 Boundary condition of mathematical models

The wall boundary condition was used for PKW and bottom wall while the inlet was kept as velocity-inlet. Volume fraction at the inlet was specified as water being one and air being zero. The wall boundary was given a no-slip boundary condition, while the standard wall surface function was used to model the areas near the wall. The top portion of the channel and outlet portion was given a pressure outlet condition with no backflow of water. The sides of the channel were given a symmetry boundary condition. The mathematical model after assigning the governing equations and boundary conditions is complete.

3.5 Discretization Error and Numerical Solution Strategy

The mathematical model using the FVM in ANSYS Fluent requires splitting our domain into multiple control volumes or cells. FVM uses the integral form of these governing equations rather than the differential form.

The governing equations are satisfied in each cell of the domain, and the values of unknowns are determined at the cell centers of each cell. Discretization means determining unknown functions of selected variables at these selected points. The problem at hand thus reduces to finding cell center values to a fixed number of cell centers.

The cell centers values obtained as such are interpolated to get values at control surfaces, while boundary conditions (BCs) are provided at the edge of the domain of the control volume. Each of these algebraic equations relates a cell center value to its neighbors, and these algebraic equations are solved by inverting it on the computer to get the cell center values of unknowns we want to find.

This averaging and interpolation of the cell center values to get values at control surfaces introduces an error in this process. The error introduced in going from the integral form to the set of algebraic equations is called the discretization error. This discretization error can be reduced by using more cells in the domain, i.e., mesh refinement or increasing the order of accuracy of the interpolation.

Though the conservation is guaranteed in FVM, but there are interpolation errors which is unavoidable. But even on a coarse mesh, like this, the interpolation errors don’t lead to spurious nonphysical results, such as mass accumulating or mass disappearing from a control volume or mass leaving a control volume doesn't match the mass entering the adjoining control volume, which could be the case in the finite element method.

The control volume balance for mass and momentum helps derive a system of algebraic equations in each cell of the mathematical model constrained by boundary conditions. The numerical solution strategy is depicted in Fig. 3.3 below.

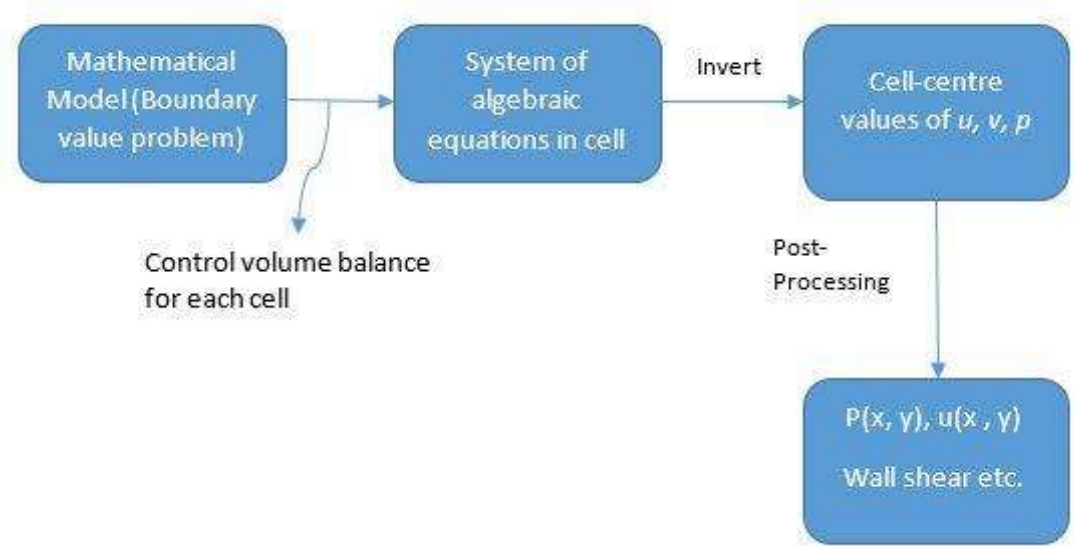

Figure 3. 3 Numerical solution strategy (Courtesy of A Hands-on Introduction to Engineering Simulations (edX) by Dr.Rajesh Bhaskaran)

3.6 Advantage of FVM Method Over Other Methods

An essential advantage of the finite volume method is that conservation is built into the method. The mass and momentum conservation equations are conserved in each cell. FVM here differs from FEM in the methodology used to derive these systems of algebraic equations. In FEM control, volume balance is not performed in each cell. It is instead done by weighted integral form and using polynomial interpolations.

The Finite Difference Method (FDM) is also a differential form of the governing equations, where partial differential equations are directly converted to algebraic equations, but this method has one disadvantage: it cannot be easily extended to irregular meshes and complex domains. Most CFD problems like our present study involving flow around Piano key Weir involve complex domains and complex geometries. As such, in real engineering applications, FDM is seldom used in CFD codes. An overview of the discretization process followed in FVM and FEM is illustrated in Fig. 3.4 below.

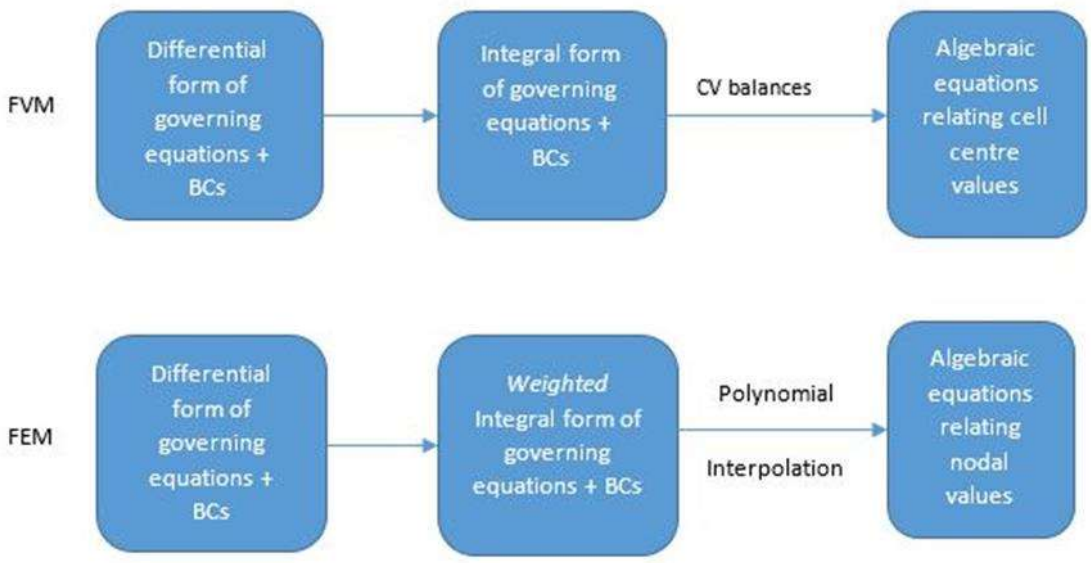

Figure 3. 4 FVM vs. FEM Models (Courtesy of A Hands-on Introduction to Engineering Simulations (edX) by Dr. Rajesh Bhaskaran).

3.7 Linearization Error and Deriving the System of Algebraic Equations

The system of algebraic equations derived by the FVM Method of control volume balancing has an additional complication. The additional complication refers to the algebraic equations being nonlinear.

As seen in the integral form of the momentum equation in Table 3.1, there is a nonlinear term. This nonlinear term is a product of two unknowns, i.e., the product of velocity times a velocity component. This set of nonlinear system of algebraic equations is solved by linearizing the nonlinear terms about some guess values, which introduces a new error called Linearization error. The CFD solver iterates the values around the guess values, updating the guess at each time. The iteration converges to give a good solution to the set of nonlinear systems of algebraic equations.

To decrease the linearization error, the CFD solver has to solve iteratively. The solver, after each iteration, updates the guess values until imbalances of mass and momentum are below some selected tolerance, and this linearization error becomes acceptable. Fig.

3.5 illustrates the iterative algorithm for the solution.

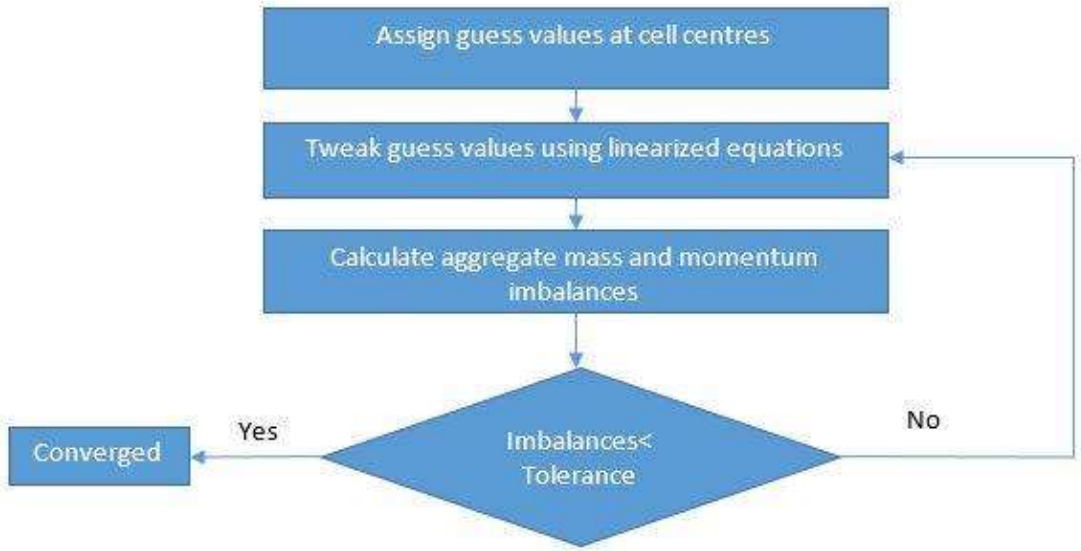

Figure 3. 5 Algorithm for iterative solution (Courtesy of A Hands-on Introduction to Engineering Simulations (edX) by Dr.Rajesh Bhaskaran)

Simply refining the mesh does not tend to decrease the overall error.

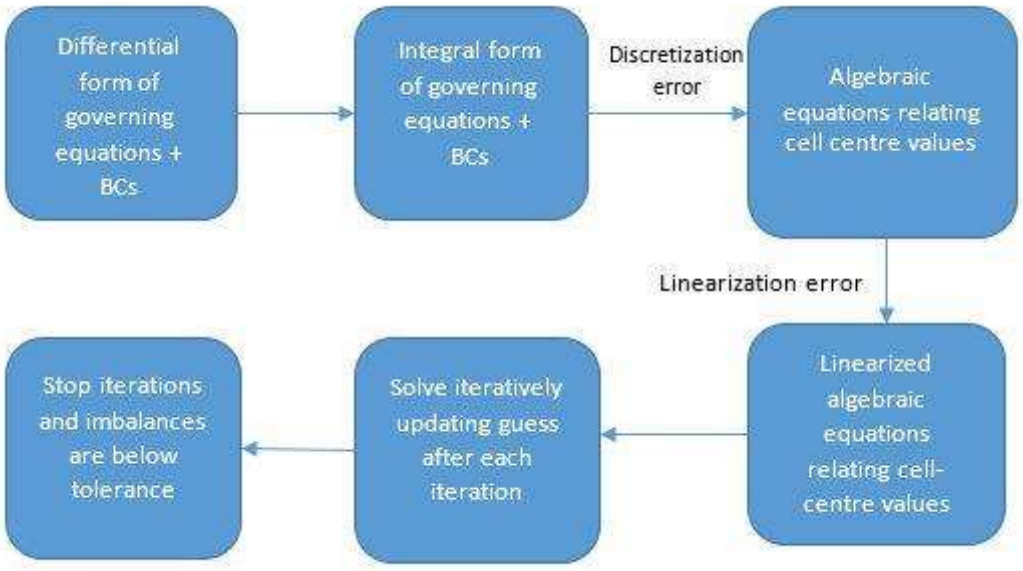

Figure 3. 6 Steps of numerical solution (Courtesy of A Hands-on Introduction to Engineering Simulations (edX) by Dr.Rajesh Bhaskaran)

The finer mesh makes the iterations harder to converge. Decreasing the discretization error makes the linearization error high, and as such, a balance between the two has to be maintained for getting an optimal solution through the CFD solver. The numerical solution steps are presented in Fig. 3.6.

3.8 Verification and Validation of the Numerical Study

Verification of the numerical model involves checking the mathematical model for numerical errors, comparison with hand calculations, mass and momentum imbalance check and as well as obvious trends as established by previous researchers.

Validation of the numerical model is checked by comparing the numerical results with experimental data.

*****

CHAPTER 4 NUMERICAL STUDY OF DISCHARGE-HEAD RELATIONSHIP OF PIANO KEY WEIRS FOR LOW HEADS

4.1 Introduction

Existing hydraulic structures need to be updated from time to time due to rising flood levels. Adding spillway capacity in the original design involves loss of storage or construction of gates. An increase in reservoir storage can be accomplished either by improving the embankment crest or adding fuse plugs that are limited to only new constructions.

The research was carried out to increase the length of the weir crest from time to time, and as a result, 'labyrinth weir' was conceived and designed. The research was undertaken to optimize the geometrical parameters of the weir affecting the discharge so that the construction cost can be minimized. However, labyrinth weir presents difficulty if the footprint requirement is not available on existing dams.

The PKW is not only convenient to use on most concrete and earth dams, which are already equipped with a free flow spillway but also serves as an excellent alternative to increase further the discharge capacity of existing as well as new dams (Leite Ribeiro et al. 2009; Lempérière and Ouamane 2003).

The efficiency of a PKW is often compared with a linear weir since the PKW behaves as a linear weir at a higher head. Therefore, increased discharge is often expressed by ratio r of the discharge Q_{PKW} through PKW and discharge $Q_{.W.}$ of a linear weir with the same width W (Ribeiro et al. 2007).

$$r = Q_{PKW}/Q_W \tag{4.1}$$

Kabiri-Samani and Javaheri (2012) conducted extensive experiments to find the head-discharge relationship of PKW both in free flow and submerged flow conditions.

After regression of experimental data, Kabiri-Samani and Javaheri [12] obtained the

following relation for the Coefficient of discharge C_d for free flow.

$$C_d = 0.212 * \left(\frac{H}{P}\right)^{-0.675} * \left(\frac{L}{W}\right)^{0.377} * \left(\frac{Wi}{Wo}\right)^{0.426} * \left(\frac{B}{P}\right)^{0.306} * e^{(1.504\left(\frac{Bo}{B}\right)+0.093\left(\frac{Bi}{B}\right)} + 0.606 \quad (4.2)$$

The above equation is valid under following conditions (i) H >30 mm, (ii)0.1 ≤ H/P ≤ 0.6, (iii)2.5 ≤ L/W ≤ 7, (iv)1 ≤ B/P ≤ 2.5, (v)0.33 ≤ W_i/W_o≤ 1.22, (vi)0 ≤ Bi/B ≤ 0.26, (vii) 0 ≤ B_o/B ≤ 0.26 and (viii) H_d/H ≤ 0.6 .

The discharge through PKW is calculated using a sharp-crested weir as below: -

$$Q = \frac{2}{3} C_d \sqrt{2g}\, LH^{1.5} \quad (4.3)$$

Here the exponent over the H is proposed to be 1.5 when H>30 mm, and therefore, surface tension force can be neglected.

Exponent over the crest-head (*h*) was interestingly observed to be 0.75 in the experiments done by (Tiwari and Sharma 2017a) on PKW for h/P <0.1 and developed length ratio L/W equal to 4.76 in a 0.5 m wide rectangular channel. Discharge Head relationship was observed as below:

$$\frac{Q}{LW} = C_d h^{3/4} \quad (4.4)$$

Where '*h*' is the head over the crest of the PKW. The Coefficient of discharge C_d by regression modeling was found to be 0.715.

CFD modeling, along with physical modeling or composite modeling, is gaining popularity as the most effective tool for analyzing flow problems. CFD studies have long been carried out to replicate experimental results, and even simulations on different numerical models have led to the finalization of a physical model. CFD studies of weirs have long been undertaken in the past to study the flow behavior around

them (Erpicum et al. 2012; Fleit et al. 2017; Haun et al. 2011; Muslu 2001). CFD study of labyrinth weirs with large side angles has been undertaken to study the flow pattern around them (Carrillo et al. 2020).

Various authors have also undertaken CFD studies of the head discharge relationship of PKW since its inception. Erpicum et al. (2011a) conducted studies on PKW within its operational head-range by 1D numerical modeling.

Hu et al. (2018) did a comprehensive numerical study for flow around PKW and suggested various parameters affecting the side crest and discharge efficiency of PKW for the head kept at a minimum of 50 cm. Eng and Lennart (2018) suggested that finer mesh in the numerical model gives velocity values closer to experimental value, and the discharge coefficient can be calculated more accurately.

Abrari et al. (2015) conducted their numerical studies for the discharge capacity of PKW as a function of the various inlet to outlet width ratios with a minimum crest head of 30 cm and proposed an equation for discharge coefficient. However, the minimum head was 30 mm. Oertel (2015) compared the investigated discharge from physical laboratory models with numerical 3D and found a good agreement between the results with Anderson and Tullis (2012b) for $H/P > 0.15$ where H is the total head at a sufficient distance upstream of PKW.

In all of these numerical simulations, nappe height was kept at more than 30 mm so that surface tension force could be neglected. Numerical study of head-discharge relationship over an entire set of discharges with h/P ranging from 0.04 to 0.1 as such is not available. The primary objective of this study is to conduct the numerical simulation of the head discharge relationship using ANSYS FLUENT for such small discharges and validate the experimental result of Tiwari and Sharma (2017a). Half key geometries of the physical model used in this experimental work have been used for

simulating the flow around PKW (Fig. 4.1 (a)). The numerical simulation incorporates the effect of surface tension force modeling as the nappe height is less than 30 mm. The streamlines for a few discharges have been shown, and the nature of flow for such small discharges is compared.

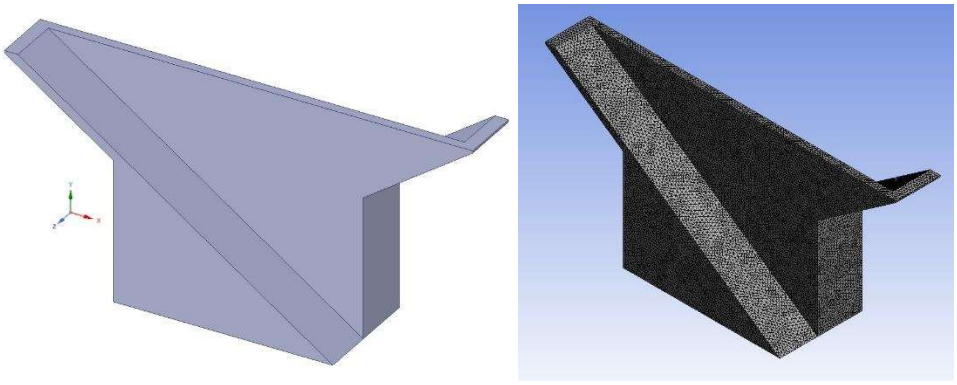

(a) **(b)**

Figure 4. 1(a) Half PKW model for numerical study (b) Finer mesh for PKW

4.2 Governing Equations

ANSYS FLUENT solves mass and momentum conservation equations for all flows.

$$\frac{\partial \overline{u}_j}{\partial x_j} = 0 \tag{4.5}$$

$$\rho\left(\frac{\partial \overline{u}_i}{\partial t} + \overline{u}_j \frac{\partial \overline{u}_i}{\partial x_j}\right) = -\frac{\partial p}{\partial x_i} + \frac{\partial}{\partial x_j}\left(\overline{\tau}_{ij+}\overline{R}_{ij}\right) \tag{4.6}$$

Where, ρ = density of water; p = pressure; t =time; $\overline{u_i}$=mean velocity in x_i direction; $\overline{\tau_{ij}}$ = mean viscous stress tensor; and $\overline{R}_{ij}$= Reynolds stress tensor (i, j=1, 2, 3) defined as:

$$\overline{R}_{ij} = -\rho\overline{u_i' u_j'} \tag{4.7}$$

Using Boussinesq's eddy-viscosity concept, the $\overline{R}_{ij}$ can be written as

$$\bar{R}_{ij} = \rho \varepsilon_m \left(\frac{\partial \bar{u}_i}{\partial x_j} + \frac{\partial \bar{u}_j}{\partial x_i} \right) \quad (4.8)$$

The proportionality ε_m is called eddy viscosity, and it has a dimension similar to kinematic viscosity ν used as the proportionality constant for defining the mean viscous stress tensor.

$$\bar{\tau}_{ij} = \rho \nu \left(\frac{\partial \bar{u}_i}{\partial x_j} + \frac{\partial \bar{u}_j}{\partial x_i} \right) \quad (4.9)$$

The k equation for the realizable model is the same as that of the standard model or the RNG model, but the model constants are different. However, the dissipation rate equation (ε) is substantially different and is better as the transport equation does not have any term containing singularity as in the traditional k-ε model. Model constant C_μ is also not constant but variable, unlike in the standard model.

Typical default values of the constants in the realizable k-ε model are

$C_{1\varepsilon}$=1.44, C_2 =1.9, σ_k =1.0, σ_ε =1.2

Where σ_k and σ_ε represent the Turbulent Prandtl numbers for k and ε.

The default values are adopted for the model as the constants have been established to ensure that the model performs well for canonical and asymmetric jets as per ANSYS Manual.

Numerical simulation on the above experimental model features half key geometries (Fig. 4.1(b)) with transient pressure-based simulations with Realizable k- ε for open channel flow over hydraulic structures like PKW. Computational fluid dynamics (CFD) simulation using FLUENT solver is selected for our numerical study for flow over half unit PKW with dimensions, as shown in Table 4.1. The free surface level has been measured at the crest level of PKW.

Table 4. 1 Dimension of the numerical model (All units in mm) (adapted from experiments by Tiwari and Sharma (2017a)

Sl No.	W	B_i	B_o	P	W_i	W_o	B_b	T_s
1	84	80	80	160	38.5	5	7	7

4.3 Three–Dimensional Numerical Model

The physical PKW model was taken from experiments done by Tiwari and Sharma (2017a) on PKW with symmetrical overhangs and the same inlet and outlet widths. The discharge and the corresponding head observed over the PKW crest were taken from the Literature for our simulation process.

4.3.1 Meshing and Boundary Condition

The water inlet boundary was located at a sufficient distance (~ 19 P) for developing uniform flow conditions for the above numerical study. PKW was meshed with a 2 mm element size (Fig. 4.1(b)). In total, approximately 1.6 million elements represent the model area. For the Grid independence study, finer cells of 1.5 mm were used, and the meshing resulted in about 2.2 million cells. The water inlet boundary condition was set as ‘velocity inlet’ as per the discharge flowing in the Channel. The volume fraction at the inlet was specified as water is one, and the air is zero. The top boundary and the outlet of the channel flow were set as a pressure outlet boundary with zero-gauge pressure and backflow volume fraction of air as one and zero for water. The bottom of

the Channel was set with no-slip wall boundaries. Each simulation in the present numerical study was run for a different number of time steps along with different time step sizes, which varied from 0.0005 to 0.1second for different discharges, with the minimum flow time being 30 seconds for a stable flow. Water flow was considered incompressible, and the default standard density and viscosity of water at 20°C were used in all calculations. Also, since the head is quite small and less than 30 mm, phase interaction was selected, and surface tension was also modeled in the numerical study. The model was run on a 64GB RAM INTEL XEON Processor with 20 Cores.

4.3.2 Numerical Algorithm

The authors have used the Volume of Fluid (VOF) model with two Eulerian phases (water and air) with sub-model as open channel flow with the implicit formulation and implicit body force. Transient modeling was adopted for the simulation process. However, Transient flow simulations are more time-consuming and challenging than laminar flows in many ways. Additional equations of the turbulence quantities are solved for Reynold's averaged approach. Also, the realizable (k-ε) model is used in the present study as the viscous model to simulate the effect of turbulence. The realizable model contains a new formulation for the turbulent viscosity and a different transport equation for the dissipation rate (ε), which is derived from the exact equation for the transport of the mean square vorticity fluctuation. Realizable implies that the model satisfies the mathematical constraints for Reynold's stresses, which is consistent with Turbulent flow physics. Both the realizable and RNG models show greater accuracy over the standard model whenever the flow consists of strong curvature, rotation or vortices. The study suggests that the realizable model demonstrates a superior ability to simulate flows involving separation and complex secondary inflows.

Pressure implicit with split operator (PISO) algorithm was selected for Pressure-Velocity Coupling Method as this algorithm is highly recommended along with neighbor correction for solving all transient flow calculations that use a larger time step. PISO algorithm gives stable results even with a relatively higher time step and under relaxation factor. Surface Tension modeling has been incorporated in the numerical model since the head is less than 30mm.

4.3.3 Verification of the Numerical Study

The head vs. experimental discharge data has been used to compare the numerical result for a large number of discharges**.** The numerical result was in close agreement with the experimentally found head vs. discharge relationship by Tiwari and Sharma (2017a). The maximum error percentage for the lowest discharge was high but under 10%. This may be due to human error while measurement of discharge and also the numerical study not being done in a natural environment.

4.4 Results and Discussion

The scaled residuals dropped well below the second order of magnitude (10^{-2}) for discharges. They remained steady while other residuals in Z-velocity, k, ε and volume fraction (air) dropped to the fifth order of magnitude (Fig. 4.2(a)). Since the mean quantities and the turbulent quantities equations are strongly coupled in a highly non-linear fashion, more computational effort is required for a converged turbulent solution than for a converged laminar solution. After that, the residuals attained a constant value. Iterations varied from 20 to 50 iterations per time step size.

4.4.1 Head Discharge Relationship

The numerical result shows that the calculated head is in close agreement with that of

the experimental result for h/P <0.1. Results from the numerical model are close to those collected from the experimental model. Free water surface levels were calculated from the plotting of the iso-surface in the numerical study. For all PKW numerical models, the X-Y plane at the mid-section of the sidewall was created, and water surface elevation (head) was measured from the top of the sidewall. The head at four points was investigated along the crest of PKW by the use of the ANSYS Probe tool, and their mean values were considered. However, the best result was obtained at the mid-section of the lateral crest level of PKW.

Fig. 4. 2(b) gives a comparison between the numerical result with the experimental values. It can be shown that the numerical CFD model using FLUENT with the VOF method can be used to simulate the flow pattern upstream of PKW, allowing further studies to be taken up around PKW structure like the turbulent zone at the inflow area. The variation in head values at discharges owe to fluctuations in flow while recording data sets and the numerical study being not entirely able to simulate the natural environment of the physical model.

The numerical result also showed a good correlation with the discharge capacity formula given by Equations 4.2 & 4.3, even for heads less than 30 mm if the ‘h’ is head at the crest and not the total upstream head of PKW. This may be due to our discharge being small and h/P less than 0.1. As the discharge increases, the head given by Equations 4.2 & 4.3 tends to be more significant for that given amount of discharge since it is the total head at the upstream rather than the piezometric head at the crest.

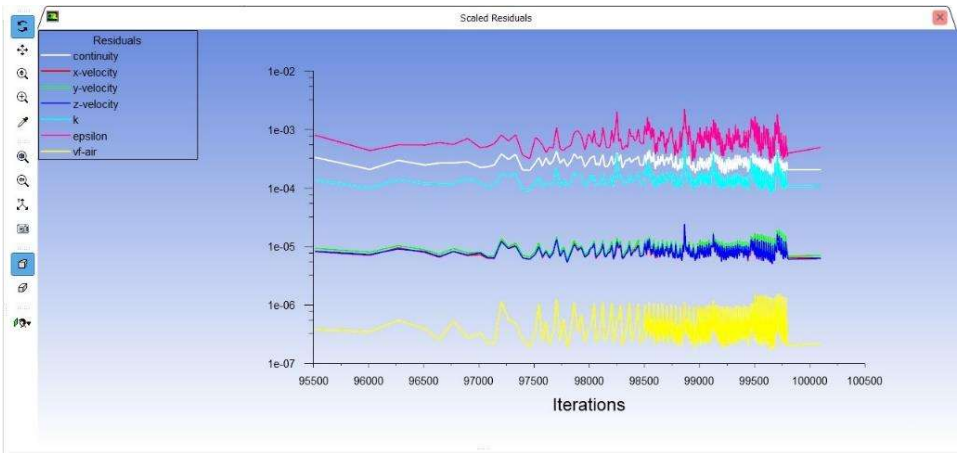

(a)

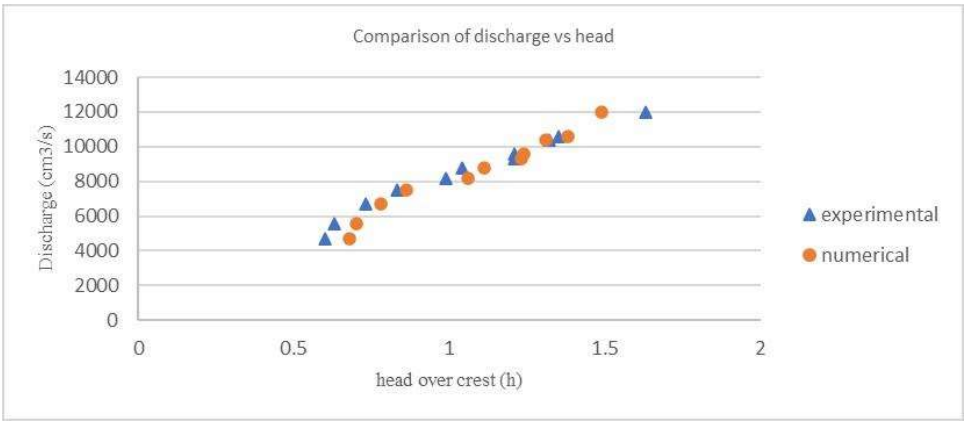

(b)

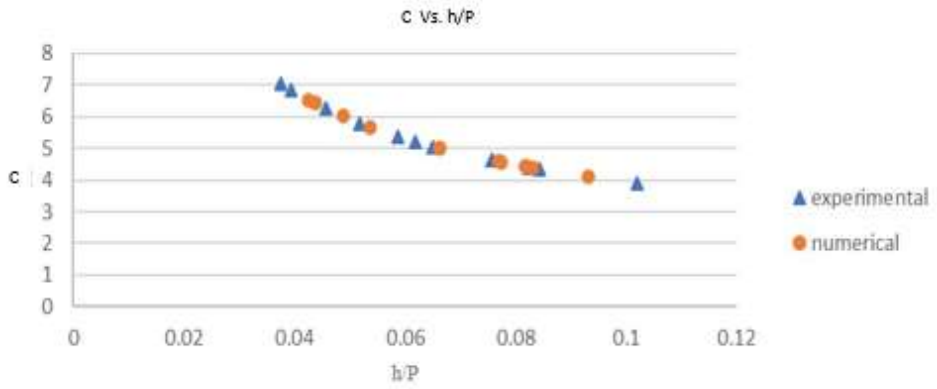

(c)

Figure 4. 2(a) Residuals for the numerical study at a discharge (Q) of 4700cm^3/s (b) Head discharge relationship between the experimental and numerical model & (c) Discharge coefficient vs. h/P plot using Eq. 7.

4.4.2 Discussion on Discharge Coefficient

The discharge coefficient (C) of numerical study has been obtained using Equation 4.3, with the head term being the head over the crest of PKW, plotted and compared for different h/P values of the experimental study for the same head. The Coefficient of determination (R^2) was found between C and h/P value using Equation 4.3 for both experimental and numerical value of head. The linear trend line pattern gave an R^2 value of 94.21 for the experimental value and 97.46 for the numerical values suggesting the numerical study is in close agreement with the experiment study and follows the same trend line. The discharge coefficient, as observed, is much higher than traditional weirs, such as rectangular weir, which has a discharge coefficient in the range of 0.6. Labyrinth weirs have higher values but not as high as PKW. The authors observe that the discharge coefficient (C) decreases as the h/P value increases (Fig. 4. 2(c)), which is consistent with the Literature. The numerical study undertaken supports the experimental result that Equations 4.2 & 4.3 can be used for low heads if the head is measured at the crest of PKW.

4.4.3 General Water Surface Profile Observations

The flow over PKW consists of two discharging portions: one, which is spatially varied flow along the lateral crest of PKW from inlet falling to the outlet and second, which is a normal jet flow over the upstream and downstream apexes. For low heads, as in our numerical study, the lateral nappe profile almost remains depressed up to the discharge of 7500 cm^3/s. When the discharge reaches a value of 10000 cm^3/s, the nappe becomes free at the lateral crest but still clings to the sidewalls later (Fig. 4. 3(b)). The nappe profile at the downstream inlet changes from clinging to leaping to springing nature as the H/P ratio increases from 0.15 to 0.35 (Machiels et al. 2009). As such, the general

nappe profile around PKW for H/P less than 0.1 is that of depressed flow and is supported by our CFD study. The water surface profile sticks to the hydraulic structure (Figs. 4. 3(a) & 4. 3(b)). Streamlines were also plotted along the length of PKW (Fig. 4. 3(a)), which gives a glimpse into the water surface profile near PKW. The water surface flow sticks to the structure at the downstream inlet portion but dips at the beginning of the lateral crest of PKW.

As the head increases over PKW, the control section moves from the downstream crest of the inlet to the upstream side. This causes the water surface profile to become a rippled profile instead of a flat profile (Erpicum et al. 2012). However, since, in our case, the head is so small, the water nappe profile is of a flat one (Fig. 4. 3).

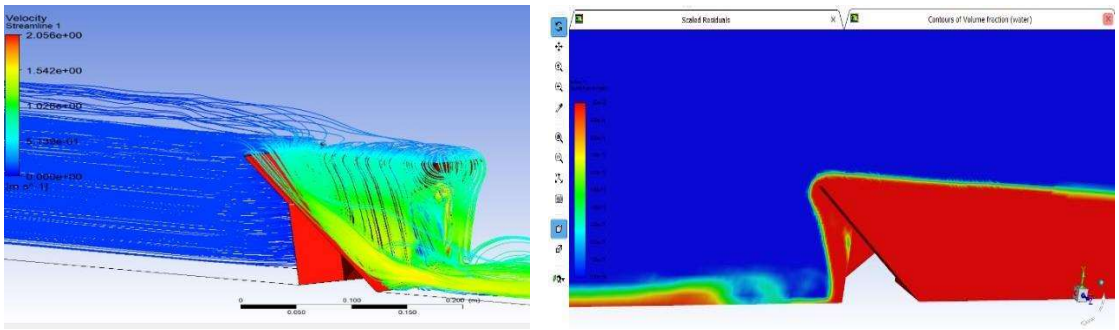

(a) (b)

Figure 4. 3(a) Nappe profile over the crest of PKW for a discharge of 10600 cm^3/s

(b) Water flow profile for a discharge of 10600 cm^3/s

Further, PKW is a structure that is said to be self-aerating and self-cleaning structures. For accessing the self-aerating nature of PKW, the Probe tool for pressure at the inlet and outlet portion of PKW was used, and the study indicates no negative pressure suggesting fairly good air entrainment and no danger of cavitation in the studied discharges. The self-cleaning aspect of PKWs can be observed by studying the velocity profile upstream of PKW

4.4.4 Velocity Distributions

Open Channel Hydraulic research is dependent on its velocity distribution from bed to surface. Velocity distribution profiles are generally used for the design of channel cross-section, hydraulic structures and analysis of sediment transport.

By the use of CFD, we will see the longitudinal velocity profiles ('u') along the Channel at different depths of open channel flow. Two cross-sections distances of 150 mm(X1) and 450(X2) mm from the upstream apex of PKW were selected for observing the velocity components. At each cross-section, five depths (Y1, Y2, Y3, Y4 and Y5) were chosen to study velocity at different depths of the cross-section at a distance of 3 cm, 6 cm, 9 cm, 12 cm and 15 cm, respectively, from the bed level. Also, two points along the Z direction, one at the middle portion of key (Z1) and the other in front of the sidewall (Z2) of PKW, were chosen for study purposes.

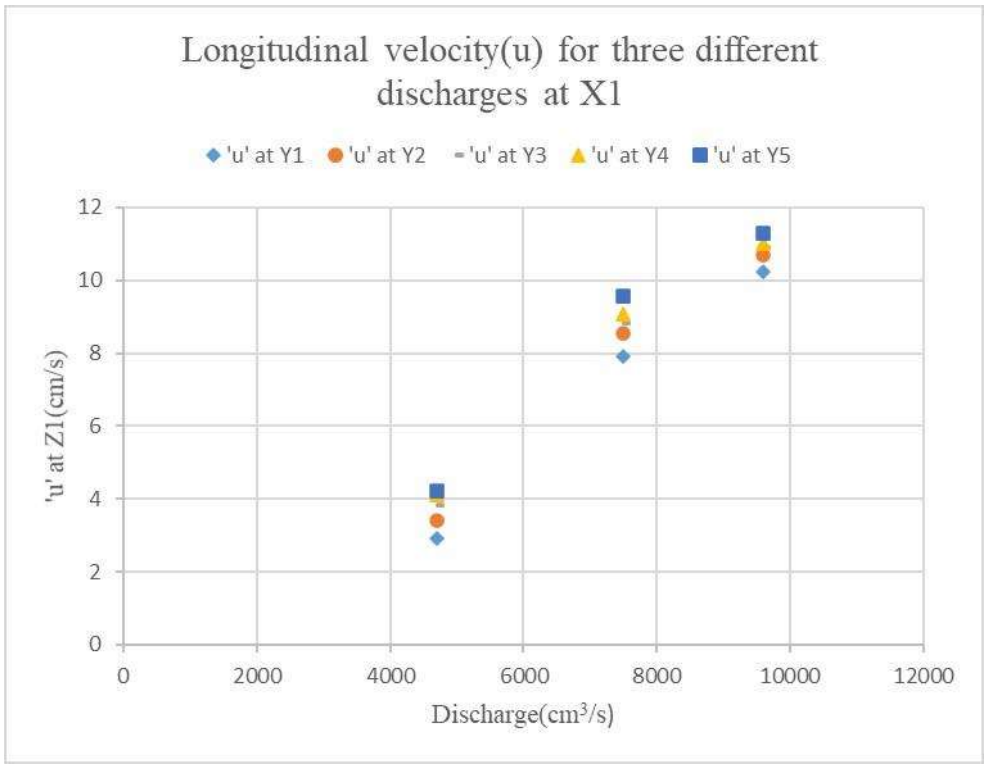

(a)

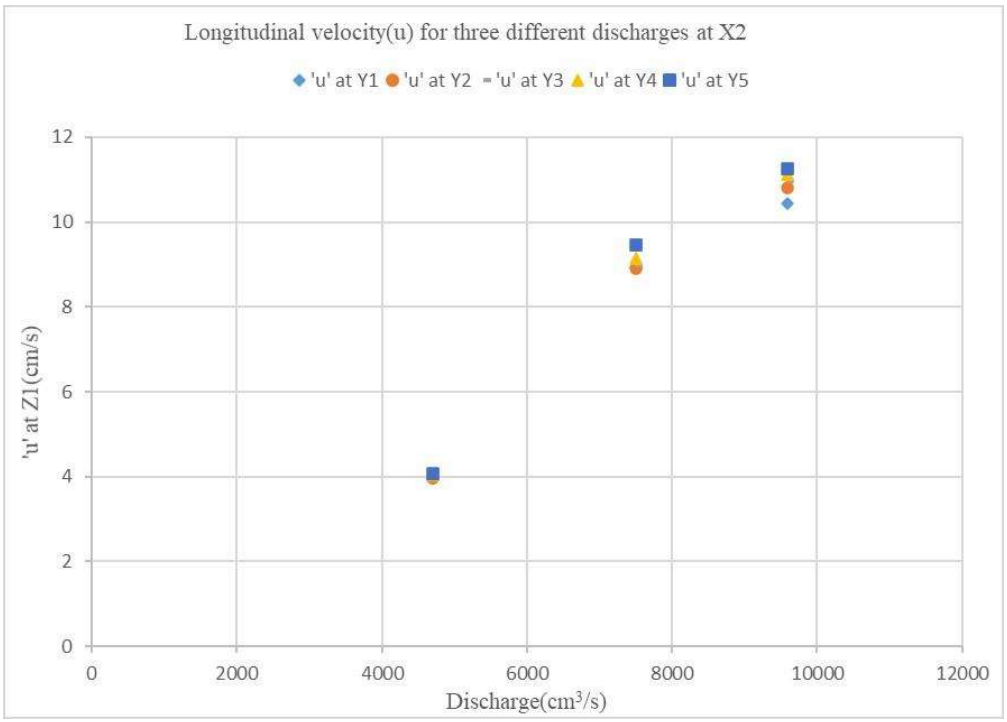

(b)

Figure 4. 4(a) Longitudinal velocity (u) for three different discharges at X1 and Z1

(b) Longitudinal velocity (u) for three different discharges at X2 and Z1.

Longitudinal velocity (u) is utilized by sediment particles to move downstream. CFD study shows that the longitudinal velocity increases as we move away from the PKW. Further higher discharges have higher longitudinal velocity. PKW being a hydraulic structure decreases the longitudinal velocity in its vicinity while allowing water to pass over it. The longitudinal mean velocity (u) for open channel flow at two different cross-sections and three different discharges is shown in Fig. 5.6 above. The longitudinal velocity (u) can be observed to be more closely spaced and uniform for cross-sections closer to PKW at different X.Z. planes as we move farther from PKW.

4.5 Conclusions

Due to larger floods, the existing structures are at risk and not being able to safely pass the flood downstream, leading to overtopping of hydraulic structures. However, with the advent of PKW, the discharge capacity of old existing spillways can be safely increased. PKW's are being undertaken for existing and new projects all around the world as an effective spillway dissipater.

The present numerical CFD study investigated the heads for different values of discharges and compared the results with the experimental values from Literature. It can be found that the numerical CFD model can reproduce flow depths near PKW with good agreement with the experimental model. The graph between the experimental and numerical results has been plotted, and the water surface contour plot has been shown. The numerical study suggests that the empirical equation by Kabiri-Samani and Javaheri (2012) gives good results for h/P Value <0.9 when the head is measured at the crest of the weir rather than the upstream of PKW. However, more experimental studies are necessary in this regard. The nature of flow around PKW for H/P ratio less than 0.9 is clinging in nature, as suggested by our numerical study and supported by Literature.

Streamlines have been shown for flow over PKW, and it suggests that the water level remains flat along the entire crest length of PKW as the flow enters the lateral crest length with no buildup of negative pressure at the inlet and outlet portion. The longitudinal velocity profile shows that the velocity increases as we move away from PKW.

As there are a large number of geometrical parameters influencing the flow, constructing different physical models for PKW for estimating the optimal geometric parameters required for any project design can be tedious. Present Numerical study suggests that CFD can be used as a guiding and analysis tool for investigating the hydraulic need of the various PKW projects, thus drastically lowering the time required for planning of the project.

*****